Cooperative Binding of Nitrile Moieties Within a Bimetallic Pocket: Enforcing Side-On π-Interaction With a High-Spin Nickel(II) Site

Franc Meyer,*[a] Isabella Hyla-Kryspin,[b] Elisabeth Kaifer,[a] and Peter Kircher[a]

Dedicated to Prof. Dr. Peter Paetzold on the occasion of his 65th birthday

Keywords: Cooperative effects / Coordination modes / Nickel / Bimetallic complexes / π interactions

Different cooperative binding modes of nitriles within the bimetallic pocket of a pyrazolate-based compartmental dinickel(II) site have been studied. The H_3O_2-bridged dinuclear complex **1** reacts with cyanamide to yield **4**, in which a secondary hydrogencyanamido(1–) bridge spans the two metal centers at an unusually short metal–metal distance imposed by the primary ligand matrix. In **5**, a single 2-cyanoguanidine (cnge) molecule is *N*-bound to one nickel(II) ion through its nitrile part and is coordinated to the adjacent metal site through an amido nitrogen. The characteristics of the coordination spheres of the metal centers suggest an additional side-on π-bonding interaction of the nitrile moiety with the second high-spin nickel(II) ion. This unusual interaction is corroborated by comparing the IR bands for the ν(C≡N) stretching vibration of **5** with those of complex **6**, which has two end-on bound cnge molecules, and those of the related mononuclear complex **7**, which lacks a second nickel(II) ion. The nature of the π-bonding interaction in **5** is further analyzed by DFT calculations on relevant model systems. Even though the π-bonding is found to be very weak, it does include some backbonding from occupied 3d MOs at the second high-spin nickel(II) ion to the π* MOs of the nitrile. Such an unconventional π-interaction is suggested to be enforced by the constrained fixation of the nitrile unit within the highly organized coordination pocket of the bimetallic framework. In contrast, the bifunctional 2-hydroxybenzonitrile is accommodated by the distinct binding of the nitrile and phenolate functions to the different metal centers in **8**, which confirms that the simultaneous binding of both an OR-function and an end-on bound nitrile is indeed feasible within the active site pocket. Such a situation is reminiscent of the bimetallic effect that has been assumed to enable the cooperative hydration of nitriles at the dinickel(II) site of **1**. Complexes **4**·$(ClO_4)_2$, **5**·$(ClO_4)_2$, **6**·$(ClO_4)_3$, **7**·$(ClO_4)(BPh_4)$, and **8**·$(ClO_4)_2$ have been characterized structurally by X-ray crystallography.

Introduction

The current interest in multinuclear transition metal complexes is often inspired by the occurrence of multimetallic sites within the active centers of various natural metalloenzymes.[1] The importance of such sites stems not only from their fascinating structural diversity but predominantly from their potential to enable synergetic reactivity of the adjacent metal centers.[2,3] This facilitates the generation of unusual coordination modes of small substrate molecules as well as unique organic transformations at the multimetallic framework which are often otherwise not accessible at monometallic centers. Consequently much effort has been devoted to the search for dinucleating ligand matrices that provide two (or more) coordination compartments in close proximity, in order to favor such sought-after cooperativity within the resulting bimetallic complexes.[4] With this intention in mind we recently investigated a class of pyrazolate-based dinuclear systems whose reactivity patterns can be selectively altered by appropriate changes of the chelating donor side-arms attached to the bridging heterocycle,[5] and which proved to allow novel binding modes and transformations of small molecules within the bimetallic pocket.[6,7] Among these, the dinickel(II) complex **1** (Scheme 1) has turned out to be a valuable system for the modeling of hydrolytic reactions at cooperative dinuclear sites, and, in particular, for investigating functional aspects of the metalloenzyme urease.[7]

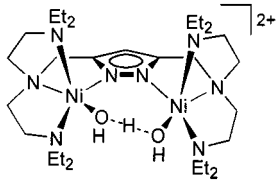

1

Scheme 1. Active dinickel(II) complex **1** (see ref.[7])

The hydration of nitriles by **1** was assumed to proceed via intermediates such as **2** (Scheme 2), in which the *N*-bound substrate has replaced a water molecule of the former intramolecular H_3O_2 bridge and undergoes subsequent nucleophilic attack by the adjacent hydroxide function to finally form a secondary *N*,*O*-amidato bridge. Alternatively, **1** may exhibit basic rather than nucleophilic behavior, as exemplified by its reaction with urea, which yields an *N*,*O*-bridging

[a] Anorganisch-Chemisches Institut der Universität Heidelberg, Im Neuenheimer Feld 270, 69120 Heidelberg, Germany
Fax: (internat.) + 49-6221/54-5707
E-mail: Franc@sun0.urz.uni-heidelberg.de
[b] Organisch-Chemisches Institut der Universität Heidelberg, Im Neuenheimer Feld 270, D-69120 Heidelberg, Germany

  1434–1948/00/0404–0771 $ 17.50+.50/0

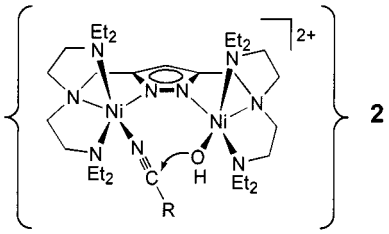

2

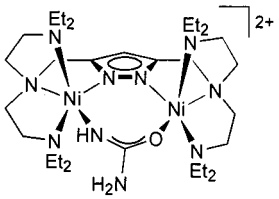

3

Scheme 2. Proposed intermediate **2** for reaction of **1** with nitriles (see ref.[7]) and urea-bridged dinickel(II) complex **3** (see ref.[6])

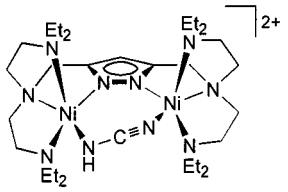

4

Scheme 3. Schematic drawing of **4**

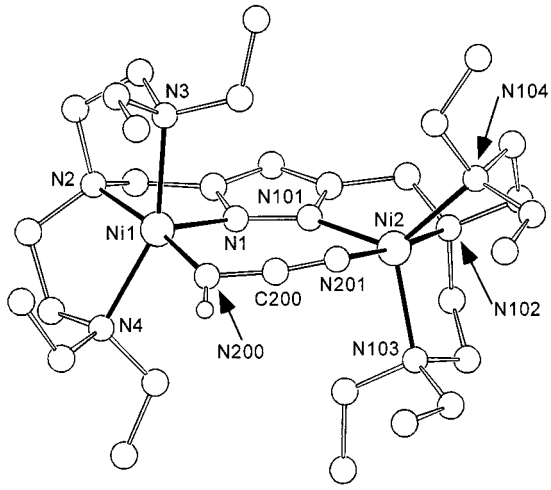

Figure 1. Molecular structure of **4**; in the interests of clarity all hydrogen atoms except H200 have been omitted; selected interatomic distances (Å) and bond angles (°): Ni1–N1 2.012(5), Ni1–N2 2.084(5), Ni1–N3 2.204(5), Ni1–N4 2.163(6), Ni1–N200 1.996(6), Ni2–N101 2.041(5), Ni2–N102 2.091(5), Ni2–N103 2.128(5), Ni2–N104 2.162(5), Ni2–N201 2.016(5), N1–N101 1.386(8), N200–C200 1.286(9), N201–C200 1.176(9), Ni1···Ni2 4.458; N200–C200–N201 172.2(7), Ni1–N200–C200 115.3(5), Ni2–N201–C200 125.9(5)

coordination mode of the deprotonated substrate within the bimetallic pocket (**3**).

In pursuit of studying such transformations mediated by **1**, we now set out to examine whether **3** would also be accessible by hydration of the appropriate nitrile, i.e. cyanamide, according to the situation depicted in **2**. Interest in this study also arose from the fact that cyanamide itself has been recognized as a substrate for both urease (yielding carbon dioxide and ammonia)[8] and Mo-nitrogenase,[9] implying its as-yet-unresolved binding to these multimetallic enzyme active sites. Unexpectedly however, several different binding modes of nitrile moieties at the bimetallic core were found in the course of these investigations, among them an intriguing coordination of cyanoguanidine (the dimeric form of cyanamide) within the clamp of the two metal ions. The present contribution describes the structural and spectroscopic characterization as well as a theoretical study of this novel system. In addition, further structural support for the postulated nitrile hydration intermediate **2** could be obtained.

Results and Discussion

When a solution of **1**·$(ClO_4)_2$ in acetone was treated with cyanamide, a crystalline green product **4**·$(ClO_4)_2$ (Scheme 3) was isolated. This compound has a strong IR absorption of the $\tilde{\nu}$(C≡N) stretch at 2149 cm^{-1} and a single ν(N–H) band at 3282 cm^{-1}. An X-ray diffraction study showed that a hydrogencyanamido(1–) bridging ligand spans the two metal centers and occupies the accessible coordination sites within the pocket of the bimetallic framework (Scheme 3, Figure 1).

The hydrogen atom of this secondary bridge could be located close to N200, which is consistent with the pronounced difference in bond lengths [*d*(C200–N200) = 1.286(9) Å; *d*(C200–N201) = 1.176(9) Å] and confirms N200 as the amido-nitrogen. Furthermore, the μ-NCN(H) proton seems to form a weak hydrogen bond with one of the oxygen atoms of a perchlorate counteranion [*d*(N200···O6) = 3.035 Å].

Obviously the characteristic property of the Ni-bound H_3O_2 unit in **1** to act as a base, which also became apparent in the deprotonation of urea to yield **3**,[6] has caused deprotonation of the cyanamide, with concomitant incorporation of the resulting $HNCN^-$ in a bridging position. The coordination chemistry of the monoanionic cyanamido(1–) ligand has attracted some attention,[10] but only one structurally characterized example of bridging parent $HNCN^-$ has hitherto been reported.[11] In that particular case, a bis(μ-hydrogencyanamido)dicopper(II) core was shown to exhibit a large metal–metal separation of 5.16 Å in conjunction with a slightly shorter C≡N bond length of 1.15(1) Å and larger angles Cu–N≡C of 146.6(8)/144.6(8)°,[11] as compared to *d*(C200–N201) = 1.176(9) Å and Ni2–N201–C200 = 125.9(5)° for **4**. This lends support for the description of the hydrogencyanamido bridge by a significant contribution of limiting form **B** (Scheme 4) at the expense of

A **B**

Scheme 4. Limiting forms of the hydrogencyanamido(1–) bridge

form **A** in the present case **4**, this apparently being imposed by the rigid pyrazolate-based ligand matrix constraining a relatively short Ni···Ni distance of 4.458 Å. The drastic decrease of $\tilde{\nu}$(C≡N) (2149 cm^{-1} versus 2256 cm^{-1} for free cyanamide) is in accord with this view.

2-Cyanoguanidine within the Bimetallic Pocket

Besides the main product **4**·$(ClO_4)_2$, a few crystals of a different product **5**·$(ClO_4)_2$ were collected from the reaction of **1**·$(ClO_4)_2$ with cyanamide. An IR spectrum indicated the presence of a nitrile unit [major absorption for $\tilde{\nu}$(C≡N) at 2154(s) cm^{-1}] as well as a series of N–H groups (several bands in the range 3200–3450 cm^{-1}) for **5**, and the elemental analysis suggested that two equivalents of the substrate were incorporated in this compound. It thus appeared that the property of the Ni-bound H_3O_2 unit in **1** to act as a base had also induced some dimerization of excess cyanamide to form dicyandiamide (2-cyanoguanidine, cnge), a process that is known to occur readily with cyanamide at pH 8–9.5 in aqueous solution.[12] Accordingly, complex **5**·$(ClO_4)_2$ can be obtained in somewhat better yields by directly treating **1**·$(ClO_4)_2$ with cnge. The overall molecular structure of **5** (Scheme 5) was resolved by X-ray crystallography, the result of which is depicted in Figure 2 and Figure 3.

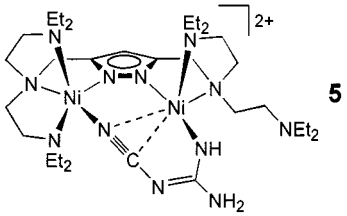

5

Scheme 5. Schematic drawing of **5**

The 2-cyanoguanidine in its deprotonated form, which is planar within 0.023 Å, is found to be coordinated to the bimetallic site in an unprecedented fashion. Its nitrile function is bound end-on to Ni2 and completes the five-coordination of the latter, which thus displays a ligation sphere intermediate between TB-5 and SPY-5, similar to the metal centers of a variety of previously characterized dinickel(II) complexes with this particular pyrazolate-based ligand framework.[5–7] On the other side the amido nitrogen atom N11 of the deprotonated cnge is coordinated to Ni1. The remaining three *N*-bound hydrogen atoms of the cnge moiety have been located as weak hydrogen bonds to oxygen atoms of the perchlorate counteranions [*d*(N11···O2) = 3.098 Å; *d*(N12···O3) = 2.973 Å; *d*(N12···O8) = 3.030 Å] with one of the latter acting as a twofold hydrogen-bond acceptor towards both N11 and N12. The equivalence of

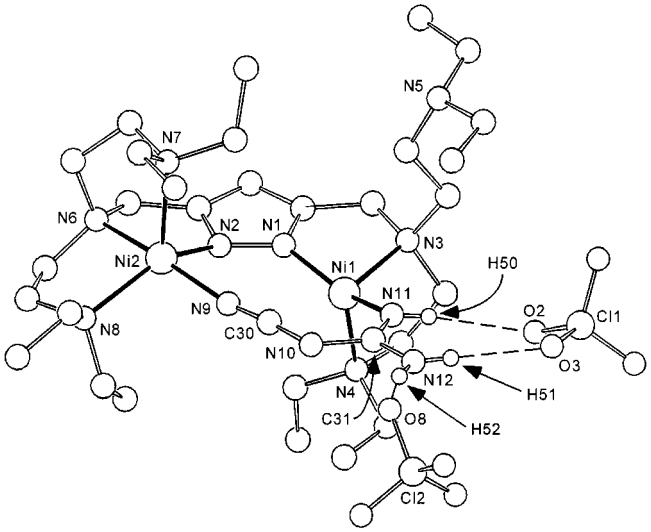

Figure 2. Molecular structure of **5**; in the interests of clarity all hydrogen atoms except those of the cnge moiety have been omitted; selected interatomic distances (Å) and bond angles (°): Ni1–N1 1.918(2), Ni1–N3 2.089(2), Ni1–N4 2.089(2), Ni1–N11 1.952(2), Ni2–N2 1.971(2), Ni2–N6 2.092(2), Ni2–N7 2.154(2), Ni2–N8 2.134(2), N2–N9 2.016(2), N1–N2 1.362(3), N9–C30 1.166(3), C30–N10 1.294(3), N10–C31 1.368(3), C31–N11 1.320(3), C31–N12 1.333(3), Ni1···Ni2 3.985; Ni2–N9–C30 171.2(2), N9–C30–N10 175.1(3), C30–N10–C31 117.8(2)

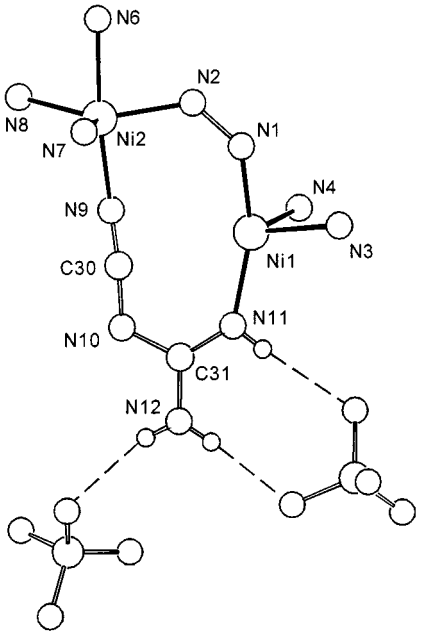

Figure 3. Representation of the central bimetallic core of **5**

the three CN bond lengths of the guanidine moiety (C31–N10/N11/N12), however, suggests the likely presence of other tautomers carrying one of the hydrogen atoms at the central N10 atom.

Unexpectedly the nitrogen donor N5 of one ligand side arm – formerly bound to Ni1 – is now found uncoordinated and dangling in **5**, which leaves the respective nickel(II) ion in a peculiar fourfold coordination environment of *N*-donors [angle N1–Ni1–N11 = 154.19(9)°] with a remaining open coordination space directed towards the inside of the

bimetallic pocket. Closer inspection of the central core of **5** (Figure 3) reveals that the nitrile moiety of the cnge – already bound end-on to Ni(2) – appears to be suitably located within the bimetallic pocket between the two nickel(II) ions to additionally interact with the low-coordinate Ni1 in a side-on fashion, even though the distances *d*(Ni1–N9) = 2.963 Å and *d*(Ni1–C30) = 2.864 Å are rather long. Some nickel complexes featuring side-on coordination of a nitrile unit have previously been structurally characterized, but these generally involve low-valent nickel(0).[13,14] Consistent with the π-backbonding ability of such low-valent nickel(0) species, the CN bonds of the η^2-bound nitriles are significantly lengthened in most of these cases, and their ν(C≡N) stretching frequencies are drastically lowered (to about 1750 cm^{-1}) relative to the free nitriles.[13] The same is also valid for nitriles bound in an η^2- or a μ-η^1,η^2(σ,π)-mode to other transition metals.[15] Cnge itself has repeatedly been used as a ligand towards transition metal ions,[16–20] in particular in copper chemistry,[18–20] and has hitherto been shown to coordinate either in a monodentate form (nitrile *N*-donor, **C**, Scheme 6) or as a bidentate bridging ligand through

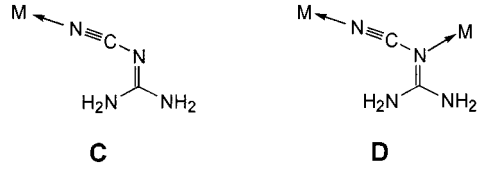

Scheme 6. Common binding modes of cnge

both the nitrile and imino-*N* atoms (**D,** Scheme 6), but not through the nitrile-*N* and a terminal amido-*N* as is observed in **5** for the first time.

The IR spectrum of cnge (both free and in coordination compounds) exhibits a characteristic doublet for the ν(C≡N) stretching vibration which has been attributed to the co-existence of different tautomeric forms of the guanidine moiety; the low-frequency component corresponds to the tautomer with conjugated C≡N and C=N bonds[21] (this single tautomer is depicted in all schemes of the present work and is used for the DFT calculations, see below). IR spectroscopic investigations of those cnge complexes of type **C** and **D** studied previously indicated that the ν(C≡N) doublet is generally shifted to slightly higher wavenumbers than free cnge ($\tilde{\nu}$ = 2205 and 2160 cm^{-1}), but that these features can hardly be used to differentiate between different binding modes of cnge.[19] It was furthermore noted that the perturbation of the IR spectra of cnge upon coordination depends more on the strength of its coordination to the metal than on the coordination type, i.e. a strongly bonded cnge showing a M–N–C angle close to 180° is expected to exhibit the most pronounced shift of the ν(C≡N) doublet to higher energy.[19] In the present compound **5** the angle Ni2–N9–C30 amounts to 171.2(2)°, but the main absorption for the ν(C≡N) stretch is found at 2154 cm^{-1} (Table 1). (Two further weak bands occur at somewhat higher energy, i.e. 2180 and 2229 cm^{-1}; it remains speculative whether these bands originate from different tautomers of the cnge fragment.) We tentatively assign the most intense band at lowest energy (2154 cm^{-1}) to the tautomer with conjugated C≡N and C=N bonds. This band exhibits a slight low-frequency shift with respect to free cnge (2160 cm^{-1}), but it is uncertain at this stage whether such a shift is to be attributed to a weak additional side-on interaction of the nitrile moiety with the second Ni1 ion. However, the observed bond length *d*(N9–C30) = 1.166(3) Å in **5** is typical for a CN triple bond and is virtually identical to the value of free cnge [1.1694(3) Å],[22] as is the angle N9–C30–N10 = 175.1(3)° in **5** [vs. 175.1(2)° in free cnge],[22] and hence there is no geometric indication of such an interaction. It should be noted, however, that geometrical changes of the N–C≡N unit upon weak side-on interaction with a high-spin nickel(II) ion should be much less distinct than in the case of a nickel(0) center due to the lower π-backbonding ability of the nickel(II) ion. Furthermore, a short atom distance for the CN triple bond (1.13 Å) has also been observed in the early crystallographic study of a substituted cyanamide π-bonded to a (carbonyl)nickel(0) fragment.[14]

In the case of two copper(I) complexes containing the cation $[Cu_2(cnge)_4]^{2+}$ with three-coordinate metal ions, the dimeric cations were found to stack in the crystal lattice in such a way that the nitrile function of a unidentate cnge molecule is located close to the axial position of a symmetry-related copper atom of a neighboring molecule.[18,19] However, the observed Cu^{I}···nitrile contacts [*d*(Cu···N) = 3.27–3.58 Å and *d*(Cu···C) = 3.50–3.65 Å][19] are much longer than those found for the present complex **5** and, consequently, any side-on binding has been judged unlikely for this copper system.[17]

Magnetic measurements performed on a powdered sample of **5**·$(ClO_4)_2$ confirm the presence of two high-spin nickel(II) ions with μ_{eff} = 3.25 μ_B per nickel ion at 297 K. The temperature dependence of the molar magnetic susceptibility χ and of its inverse $1/\chi$, as well as of the effective magnetic moment, over the range 297–5.3 K is shown in Figure 4. It reveals the absence of any significant coupling between the two metal ions (the values $|J| < 1$ cm^{-1} and g = 2.27 result from a fit of the experimental data to the

Table 1. IR spectroscopic bands for the ν(C≡N) stretch [cm^{-1}]

	KBr pellet	Acetone
4·$(ClO_4)_2$	2149(vs)	2146
5·$(ClO_4)_2$	2229(w), 2180(w), 2154(s)	2225(m), 2184(s), 2140(sh)
cnge	2205(s), 2160(s)	2184(s), 2144(w)
6·$(ClO_4)_3$	2233(s), 2186(s)	2231(m), 2184(s), 2150(sh)
7·(ClO_4)·(BPh_4)	2227(s), 2183(s)	2228(s), 2184(m)
8·$(ClO_4)_2$	2237(s)	2241

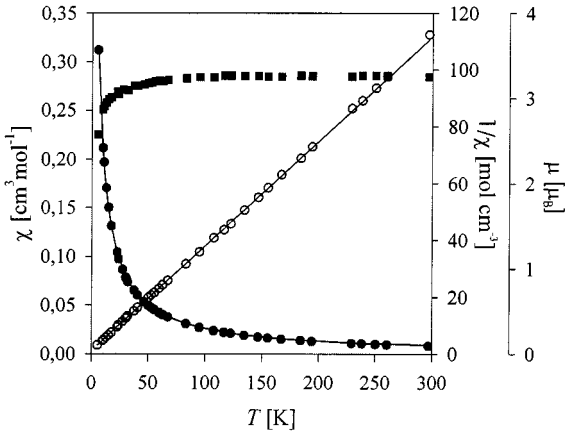

Figure 4. Temperature dependence of the molar magnetic susceptibility χ (filled circles), its inverse 1/χ (open circles), and the magnetic moment per nickel ion (filled squares) for **5**·$(ClO_4)_2$; the solid lines represent the calculated curve fits (Curie-Weiss)

standard expression for the isotropic spin-Hamiltonian $\hat{H} = -2J\hat{S}_1,\hat{S}_2$ with $S_1 = S_2 = 1$;[23] a Curie-Weiss analysis gives $C = 2.71$ and $\varphi = -3.30$).

Analogous Complexes with cnge Purely End-On Bound

In order to shed some more light on a possible contribution of the Ni1 ion to the binding of the C≡N moiety in **5**, two further complexes were investigated for comparison. The first, **6**·$(ClO_4)_3$, was obtained by treating **1**·$(ClO_4)_2$ with a large excess of cnge (Scheme 7). The molecular structure of the cation **6** as elucidated by X-ray crystallography is depicted in Figure 5.

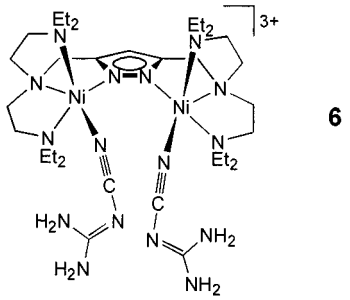

6

Scheme 7. Schematic drawing of **6**

Compound **6** features two neutral cnge ligands within the coordination pocket of the bimetallic framework, each cnge being coordinated to one of the nickel ions in a purely *end-on* fashion (type **C**, Scheme 6). The angles Ni–N–C [171.3(2) and 172.2(2)°] are basically identical to that in **5** [171.2(2)°], and, likewise, all geometric parameters of the cnge ligands in **6** are very similar to those of the cnge fragment in **5**. The cnge-bound hydrogen atoms form several weak hydrogen bonds to perchlorate counteranions or to an acetone solvent molecule included in the crystal lattice (distances N···O in the range 2.9–3.1 Å). Due to the obvious congestion caused by the binding of the two cnge molecules within the bimetallic pocket, the Ni···Ni separation is quite large (4.586 Å) and the metal ions are forced to displace rather drastically out of the plane defined by the pyrazolate heterocycle [+0.784 Å (Ni1) and –0.647 Å (Ni2)]. The exact

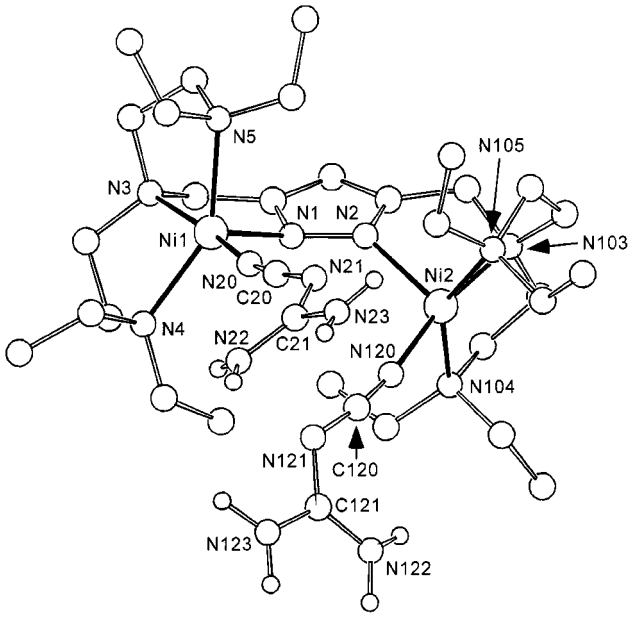

Figure 5. Molecular structure of **6**; selected interatomic distances (Å) and bond angles (°): Ni1–N1 2.035(2), Ni1–N3 2.097(2), Ni1–N4 2.125(2), Ni1–N5 2.158(2), Ni1–N20 1.983(2), Ni2–N2 2.030(2), Ni2–N103 2.097(2), Ni2–N104 2.154(2), Ni2–N105 2.137(2), N2–N120 2.000(2), N1–N2 1.389(3), N20–C20 1.162(3), C20–N21 1.295(3), N21–C21 1.334(3), C21–N22 1.325(3), C21–N23 1.329(3), N120–C120 1.152(3), C120–N121 1.304(3), N121–C121 1.338(3), C121–N122 1.331(3), C121–N123 1.331(3), Ni1···Ni2 4.586; Ni1–N20–C20 171.3(2), N20–C20–N21 170.8(3), Ni2–N120–C120 172.2(2), N120–C120–N121 172.3(3)

process leading to the formation of the tricationic complex **6** from the dicationic precursor **1** remains speculative, as no other products of the reaction could be unambiguously identified.

In order to definitely exclude any effects on the crucial ν(C≡N) vibrational frequencies caused by the distortion of the crowded bimetallic core in **6**, we prepared the corresponding mononuclear complex **7** for comparison

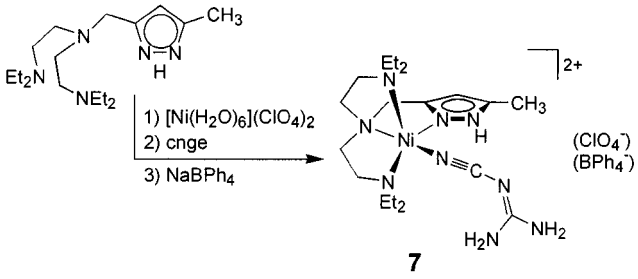

7

Scheme 8. Synthesis of the mononuclear complex **7**·$(ClO_4)(BPh_4)$

(Scheme 8). The compound **7**·$(ClO_4)(BPh_4)$ was obtained in crystalline form by treating the respective mononucleating ligand HL (that provides a single coordination compartment only)[7] with one equivalent each of $[Ni(H_2O)_6](ClO_4)_2$, cnge and $NaBPh_4$. An X-ray crystallographic analysis unequivocally confirmed the constitution of **7** as depicted in Figure 6.

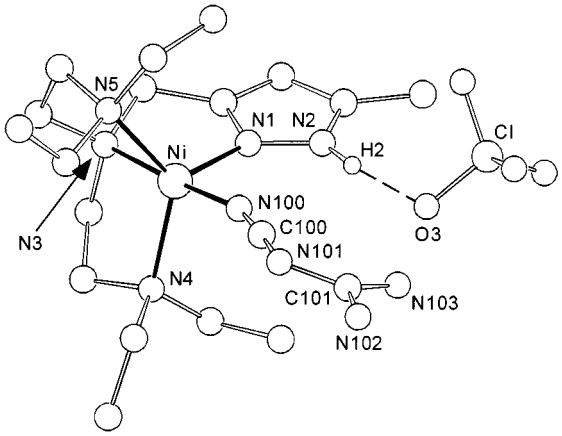

Figure 6. Molecular structure of **7** (only the major position of the disordered cnge moiety is shown); in the interests of clarity all hydrogen atoms except the pyrazole-bound H2 have been omitted; selected interatomic distances (Å) and bond angles (°): Ni–N1 1.991(3), Ni–N3 2.100(3), Ni–N4 2.105(3), Ni–N5 2.153(3), Ni–N100 1.988(4), N100–C100 1.157(7), C100–N101 1.305(7), N101–C101 1.353(7), C101–N102 1.332(7), C101–N103(7), N1–N2 1.362(4); Ni–N100–C100 163.3(4), N100–C100–N101 173.0(6), C100–N101–C101 120.8(5).

The nickel atom is nested in the tran-type coordination compartment [tran = tris(aminoalkyl)amine] and accommodates the end-on bonded cnge ligand in the remaining axial site (type **C**, Scheme 6). As anticipated, the intimate structural details of this situation closely resemble the ones observed for the nickel ions in **6** and for the Ni2 ion in **5**. The pyrazole-bound proton H2 could be located as a hydrogen bond to one of the *O*-atoms of the perchlorate counteranion [*d*(N2···O3) = 2.880 Å], where the perchlorate also forms hydrogen bonds to the terminal amino groups of the cnge [*d*(N103···O2) = 2.926 Å, *d*(N102···O4) = 2.935 Å]. Unfortunately, however, the cnge ligand was found to be disordered over two positions (ratio 85:15), and due to the moderate overall quality of the crystallographic analysis we abstain from any detailed discussion of the pivotal metric parameters of the cnge ligand.

Nevertheless, the isolation of **7** now allowed a more conclusive comparison of the ν(C≡N) stretching frequencies of free cnge with those of cnge *N*-bound to nickel(II) ions either with (**5**) or without (**6**, **7**) an adjacent second nickel(II) center, where the primary nickel(II) ions in all cases are embedded in identical pyrazolate-derived tran-type coordination environments. These values are listed in Table 1.

The complexes **6** and **7**, which feature purely *end-on* bound cnge, display similar IR bands both in acetone solution and in the solid state. As expected, their characteristic doublet for ν(C≡N) is shifted to higher wavenumbers than for free cnge. The overall differences for the low-energy component of the ν(C≡N) stretch (assigned to the tautomer with conjugated C≡N and C=N bonds[21]) are small but nonnegligible, and in the solid state a trend of decreasing frequencies in the order **6** ≈ **7** > free cnge > **5** is found. This experimental result in fact gives evidence for the presence of some (albeit very weak) side-on π-bonding interaction between the nitrile part of the 2-cyanoguanidine ligand and the proximate Ni1 ion in solid **5**. When dissolved in acetone, IR spectra in the region characteristic for ν(C≡N) are quite similar for **5** and **6**, suggesting identical structures in solution that differ from the structure observed for **5** in the solid state.

Theoretical Investigations

With the aim of further substantiating these findings, and in order to describe the electronic structure of complex **5** and to gain deeper insight into the nature of the assumed π-interaction, we have carried out DFT calculations on the simplified complexes **5a**, **7a**, and on the free ligand cnge. In **5a** and **7a** the substituents at the ligand side-arm nitrogen atoms of the parent complexes **5** and **7** have been replaced by hydrogen atoms. We started our investigations with single point calculations for the singlet, triplet, and quintuplet states of **5a** with bond lengths and bond angles taken from the X-ray data of compound **5**. Some selected results are summarized in Table 2.

Table 2. Relative energies (kcal/mol), $<S^2>$ values, atomic spin densities (ρ) and NPA charge (*q*) of the nickel atoms for the singlet, triplet and quintuplet states of **5a**

State	E_{rel}	$<S^2>$	ρNi1	ρNi2	*q*Ni1	*q*Ni2
^{5}**5a**	0.0	6.00	1.733	1.726	+1.454	+1.477
^{3}**5a**	+11.2	2.01	1.733	0.020	+1.455	+1.422
^{1}**5a**	+91.1	0.00	0.000	0.000	+1.252	+1.309

The quintuplet state of **5a** was found to be the ground state, and the states ^{3}**5a** and ^{1}**5a** lie above ^{5}**5a** by 11.2 kcal/mol and 91.1 kcal/mol, respectively. In the case of ^{5}**5a** the calculated atomic spin densities ρ as well as the NPA charges q of the nickel atoms clearly show the high-spin Ni^{II} structures. In the triplet state ^{3}**5a** the Ni2 atom adopts a low-spin configuration (ρNi2 = 0.02), while the spin density at Ni1 (1.733) remains unchanged with respect to ^{5}**5a**. The MO shapes of the metal-centered singly occupied MOs of ^{5}**5a** are shown in Figure 7.

It turns out that the singly occupied MOs of Ni1 have d_{z^2} and d_{xy} character, and consequently its three doubly occupied MOs are of $d_{x^2-y^2}$, d_{yz}, and d_{xz} character. The two latter MOs [d_{yz}, d_{xz}] are well adapted to give side-on backbonding interactions with the in-plane $\pi_\parallel$* and with the out-of plane $\pi_\perp$* MOs of the nitrile π system (Figure 8). At the same time the doubly occupied $3d_{yz}$ and $3d_{xz}$ MOs of Ni2 can give end-on backbonding interactions with the nitrogen p-component of the nitrile π* system (Figure 8). Evidently, the spatial requirements for an effective M→L backbonding in ^{5}**5a** are fulfilled and are similar to those found for Ni(0) moieties complexed to multiple π systems,[24] i.e. an electron density shift from the nickel atoms to the nitrile π* system should indeed be possible.

In order to further explore the nature and the extent of such possible backbonding interactions in complex **5** we have carried out geometry optimizations on ^{5}**5a**, ^{3}**7a**, and on the singlet state of the free cnge ligand. The optimized

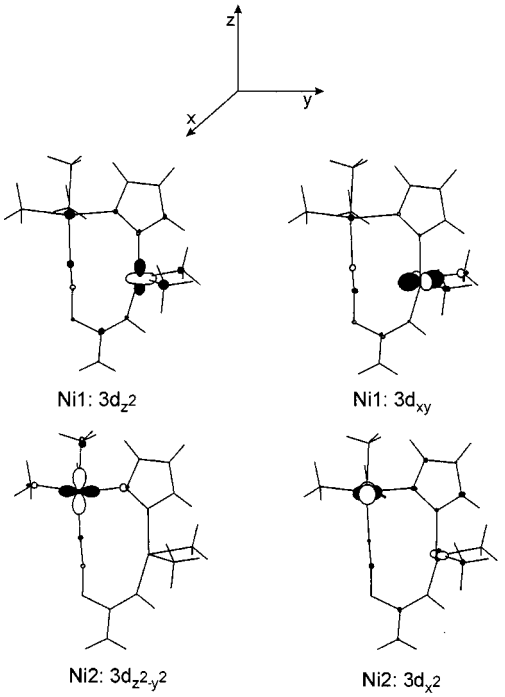

Figure 7. Shapes of the metal-centered singly occupied MOs of ^{5}**5a**

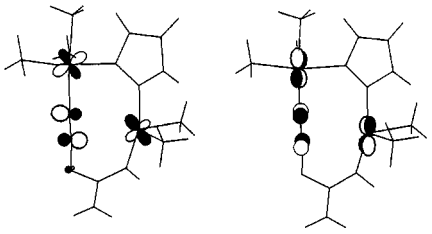

Figure 8. Possible Ni-nitrile backbonding interactions in ^{5}**5a**

structures are shown in Figure 9. According to the vibrational analyses there are no imaginary modes, and consequently these structures represent minima on the potential energy surfaces.

The optimized parameters of the free cnge molecule agree well with the known experimental data.[22] Due to the simplified nature of **5a** and **7a** some of the optimized bond lengths and bond angles differ from those determined by X-ray crystallography for the parent complexes **5** and **7** (Figures 2, 6 and 9). We ascribe these discrepancies to the spatial constraints imposed by the chelate framework of the multidentate ligands in **5** and **7**, which are not effective in the model systems **5a** and **7a**. In the case of **5a** the most striking difference is observed for the optimized Ni2–N≡C bond angle, which is 157.5° (vs. 171.2° in complex **5**). As a result, in **5a** the Ni1 atom and the N and C atoms of the C≡N unit come much closer together [*d*(Ni1–C) = 2.650 Å, *d*(Ni1–N) = 2.448 Å]. We notice, however, that the optimized Ni–N≡C bond angle of **7a** (163.9°) nicely reproduces the experimental value of the mononuclear complex **7** (163.3°). It thus seems that, in **5a**, the nitrile moiety approaches the Ni1 atom in order to enforce the side-on π-bonding interaction, while this is being prevented by the rigid dinucleating ligand matrix in the parent compound **5**.

Upon going from the free cnge ligand to **7a** and **5a**, the optimized C≡N distance increases from 1.163 Å to 1.178 Å and 1.187 Å, respectively. At the same time the calculated stretching frequency, ν(C≡N), decreases from 2209 cm^{-1} (free cnge) to 2189 cm^{-1} (**7a**) and 2143 cm^{-1} (**5a**). The trend of decreasing ν(C≡N) frequencies determined theoretically (free cnge > **7a** > **5a**) differs from that observed experimentally (**7a** > free cnge > **5a**). The calculation (for the gas phase) obviously fails to reproduce the well-known[25] increase in ν(C≡N) that occurs upon end-on binding of the nitrile (in the solid state or in solution), but it suggests that in **7a** the nitrile part of the cnge ligand receives some back-

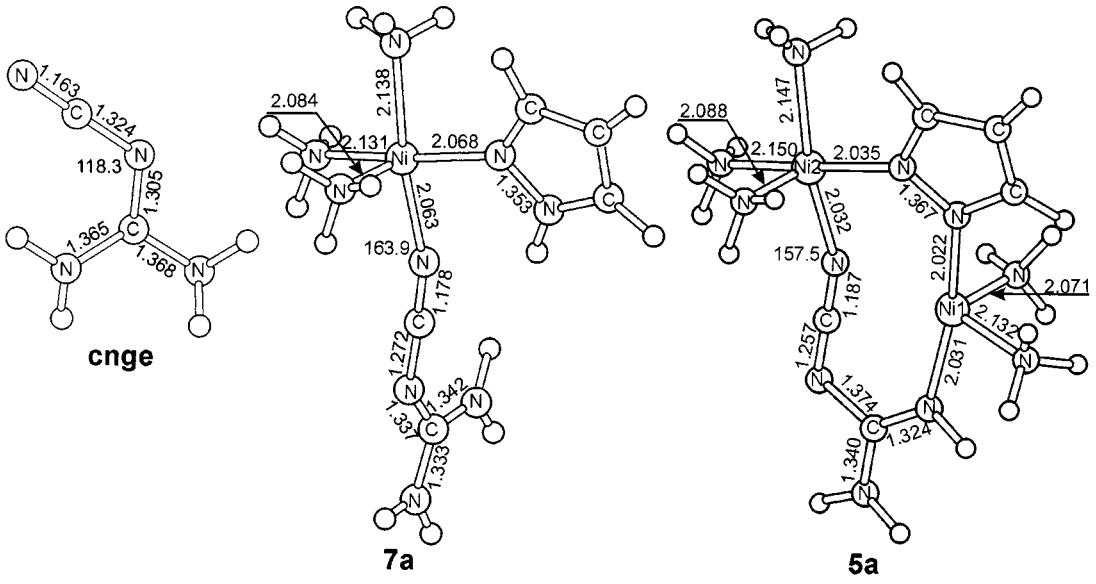

Figure 9. Optimized structures of free cnge, ^{3}**7a** and ^{5}**5a**; bond lengths are given in (Å) and bond angles in (°)

Table 3. Results of NBO and NPA population analyses, optimized C≡N bond lengths and calculated wavenumbers for the ν(C≡N) stretch of cnge, **7a**, and **5a**

	NBO occupation numbers		
	cnge	**7a**	**5a**
σ(C≡N)	1.995	1.990	1.989
π(C≡N)	3.962	3.966	3.935
σ*(C≡N)	0.023	0.029	0.025
π*(C≡N)	0.224	0.456	0.542
	NPA charge		
Ni2		+1.495	+1.477
Ni1			+1.481
–C≡N	–0.023	–0.176	–0.244
d(C≡N) [Å]	1.163	1.178	1.187
$\tilde{\nu}$(C≡N) [cm^{-1}]	2209	2189	2143

bonding from occupied MOs of the nickel ion (see Figure 8). The calculated NPA charge of the nitrile moiety changes from –0.023 (free cnge) to –0.176 (**7a**), and the population of the nitrile π* MOs increases from 0.224e (free cnge) to 0.456e (**7a**) (Table 3). We suppose that in the experimental complex **7** the end-on Ni–nitrile interactions may have a slightly different character, obviously affecting the observed ν(C≡N) stretching frequencies.

Upon going from **7a** to **5a**, an additional increase of the population of the nitrile π* MOs is discernible (Table 3), while any side-on L→M donation is negligible. With respect to **7a**, the population of the nitrile π* MOs of **5a** is greater by 0.086e. Since in the optimized structure of **5a** the Ni1 atom and the nitrile moiety come closer together than in the parent complex **5**, we also carried out NPA and NBO population analyses using the experimentally determined geometrical parameters of **5**. In this case we observe an increase of the nitrile π* MOs population by 0.049e, suggesting that in **5** the Ni1–nitrile π-bonding has to compete with the structural constraints imposed by the chelate ligands, where these constraints are enforcing a larger nickel–nickel distance and a concomitant weakening of the side-on π-interaction.

In summary, the Ni1–nitrile π-backbonding in **5** can only be characterized as a weak interaction, and this is not surprising when taking into account the large charge of the nickel(II) ion and the contracted character of its 3d shell. The positioning of the nitrile unit within the bimetallic pocket and the resulting weak Ni1–nitrile interaction in ^{5}**5a** apparently block the fifth coordination site of the Ni1 center that otherwise is occupied by an additional donor ligand in all related pyrazolate-based Ni^{II} compounds.[5–7]

Binding of 2-Hydroxybenzonitrile

The question arose as to whether the unusual binding of the C≡N moiety within the bimetallic pocket of **5** is a singular phenomenon and therefore unique to the particular nitrile cnge. We thus reacted **1**·$(ClO_4)_2$ with 2-hydroxybenzonitrile, which in its phenolate form provides a bifunctional ligand of geometric characteristics quite similar to deprotonated cnge. The resulting green complex **8**·$(ClO_4)_2$ (Scheme 9) was obtained in crystalline form, and the molecular structure of the cation as elucidated by X-ray crystallography is depicted in Figure 10.

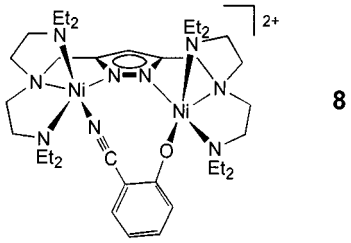

8

Scheme 9. Schematic drawing of **8**

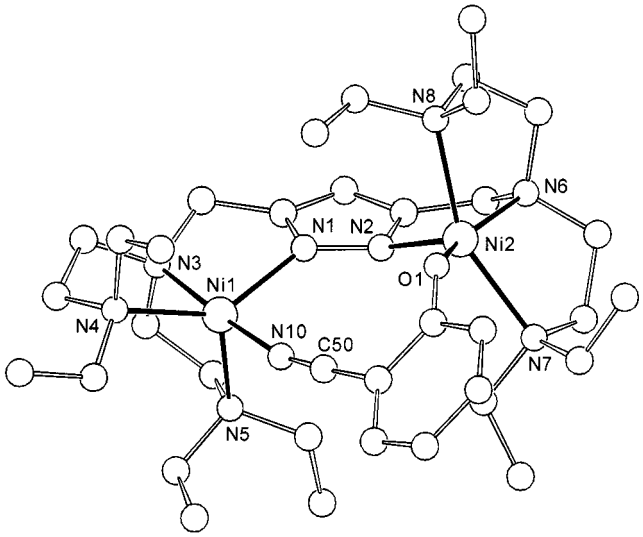

Figure 10. Molecular structure of **8**; selected interatomic distances (Å) and bond angles (°): Ni1–N1 2.050(2), Ni1–N3 2.100(2), Ni1–N4 2.172(2), Ni1–N5 2.111(2), Ni1–N10 1.988(2), Ni2–N2 2.054(2), Ni2–N6 2.087(3), Ni2–N7 2.216(2), Ni2–N8 2.208(2), N2–O1 1.934(2), N1–N2 1.386(3), N10–C50 1.135(4), Ni1···Ni2 4.587; Ni1–N10–C50 167.6(2), N10–C50–C51 176.5(3)

Obviously, the structure of **8** differs fundamentally from those of **5**. Both nickel(II) ions have retained their usual five-coordination with all the ligand side arms of the pyrazolate framework attached to the metal centers; the bifunctional 2-oxybenzonitrile(1–) ligand simply occupies the remaining active coordination sites within the bimetallic pocket. The nitrile unit exhibits plain end-on binding through its *N*-atom [angle N1–N10–C50 = 167.6(2)°] and its ν(C≡N) stretching vibration is found to be unchanged relative to those of free 2-hydroxybenzonitrile [$\tilde{\nu}$ = 2237 cm^{-1}]. These findings emphasize that particular conditions have to prevail in order to favor the weak π-bonding interaction of a nitrile unit with a nearby nickel(II) ion at the expense of the detachment of a ligand *N*-donor from the metal site, as uniquely observed for **5**.

It should finally be noted that the structure of **8** is of interest with respect to the previously proposed cooperative mechanism for the nitrile hydration mediated by **1**, which was assumed to proceed via initial end-on coordination of the nitrile to one of the nickel ions and subsequent nucleo-

philic attack by the adjacent hydroxide as shown for **2** (Scheme 2). Considering the close analogy between a metal-bound hydroxide and the metal-bound phenolate in **8**, the structure found for **8** is reminiscent of this postulated mechanism and at least demonstrates that the simultaneous binding of such an OR-function and a nitrile should, in principle, be feasible within the active site pocket of the dinuclear framework.

Conclusion

Various different binding modes of nitrile moieties at a dinuclear nickel(II) site have been characterized and studied in the present work, where the basic bimetallic framework of **1** once again proved to induce cooperative action of the two proximate metal ions. Cyanamide is incorporated as a hydrogencyanamido(1–) secondary bridge with an unusually short metal–metal separation imposed by the compartmental ligand matrix, representing only the second structurally characterized example of bridging parent $HNCN^-$. The distinct binding of a nitrile and a phenolate function at the adjacent metal centers, as observed in **8**, lends further support for the bimetallic effect that was assumed to enable the cooperative hydration of nitriles at the bimetallic site of **1**: it demonstrates that the simultaneous accommodation of both an OR-function and an end-on-bound nitrile is indeed feasible within the active site pocket of the dinuclear framework.

2-Cyanoguanidine exhibits an unprecedented binding mode within the grip of the two metal ions in **5**: while its nitrile-*N* exhibits the common end-on binding to one nickel atom, and a terminal amido-*N* is coordinated to the other metal site, the structural features suggest an additional side-on interaction of the nitrile unit with the second nickel(II) ion. Combined experimental and theoretical evidence, in particular the trend of decreasing $\nu(C{\equiv}N)$ stretching frequencies in the series **6** ≈ **7** > free cnge > **5**, as well as the proper spatial arrangement of the crucial molecular orbitals, confirm the presence of a nonnegligible (albeit weak) π-bonding of the nitrile part of the cnge ligand with the adjacent high-spin nickel(II) atom in **5**. This mainly consists of backbonding from the doubly occupied $3d_{yz}$ and $3d_{xz}$ MOs at Ni1 to the π* MOs of the nitrile. We assume that this peculiar π-bonding interaction, which is quite unusual for a high-spin nickel(II) ion nested in a purely *N*-donor environment, and which is expectedly weak, is imposed by the dinuclear pincer effect, i.e. by the seizing of the nitrile within the bimetallic pocket. Apparently, particular geometric conditions have to prevail in order to favor such side-on interaction, and this once again demonstrates the ability of two cooperating metal ions to enable unusual coordination modes by their synergetic action. One could imagine that similar interactions between π-systems and hard metal ions like high-spin nickel(II) might well play a role if enforced within highly organized and constrained substrate binding pockets, e.g. in the protein active site pockets of natural metalloenzymes.

Experimental Section

General Procedures and Methods: All manipulations were carried out under an atmosphere of dry nitrogen with standard Schlenk techniques. Solvents were dried according to established procedures. Compound **1**·$(ClO_4)_2$ and HL were synthesized according to published procedures.[7] – Microanalyses: Mikroanalytische Laboratorien des Organisch-Chemischen Instituts der Universität Heidelberg. – IR spectra: Perkin–Elmer 983G, recorded either as KBr pellets or in acetone solution. – FAB-MS spectra: Finnigan MAT 8230. – Magnetic measurement: Bruker Magnet B-E 15 C8, field-controller B-H 15, variable temperature unit ER4111VT, Sartorius microbalance M 25 D-S. Experimental susceptibility data were corrected for the underlying diamagnetism and temperature-independent paramagnetism [100×10^{-6} cm^3mol^{-1} per nickel(II) ion].[23]

Caution! Although no problems were encountered in this work, transition metal perchlorate complexes are potentially explosive and should be handled with proper precautions.

Complex 4·$(ClO_4)_2$: A solution of **1**·$(ClO_4)_2$ (0.44 g, 0.50 mmol) in EtOH/THF (1:1, 25 mL) was treated with two equivalents of cyanamide and stirred at room temperature for 2 h. All volatile material was then evaporated under reduced pressure, the residue taken up in acetone and the solution layered with light petroleum to gradually yield 0.35 g (0.40 mmol, 80%) green crystals of the product **4**·$(ClO_4)_2$. – IR (KBr): $\tilde{\nu}$ = 3282 (s), 2965 (s), 2933 (s), 2873 (m), 2149 (vs), 1467 (s), 1380 (s), 1089 (vs), 622 (s) cm^{-1}. – MS (FAB, nibeol); *m/z* (%): 779 (100) [**4**·$(ClO_4)^+$], 677/679 (98) [(**4** – 1)/(**4** + 1)$^+$]. – $C_{30}H_{62}Cl_2N_{10}Ni_2O_8$ (879.2): calcd. C 40.99, H 7.11, N 15.93; found C 41.02, H 7.13, N 15.96.

Complex 5·$(ClO_4)_2$: A solution of **1**·$(ClO_4)_2$ (0.78 g, 0.89 mmol) in EtOH/THF (1:1, 25 mL) was treated with 1.2 equivalents of cnge and stirred at room temperature for 2 h. All volatile material was then evaporated under reduced pressure and the oily residue taken up in EtOH/Et_2O (1:4, 25 mL). The green precipitate that formed was separated by filtration and dried under vacuum to afford a light green powder. This was dissolved in acetone and the solution layered with light petroleum to yield 0.16 g (0.17 mmol, 19%) of green crystals of the product **5**·$(ClO_4)_2$. – IR (KBr): $\tilde{\nu}$ = 3432 (m), 3343 (m), 3307 (w), 3232 (w), 2968 (m), 2878 (w), 2229 (w), 2180 (sh), 2154 (s), 1632 (s), 1529 (s), 1478 (s), 1468 (m), 1312 (m), 1096 (vs), 623 (s) cm^{-1}. – $C_{31}H_{64}Cl_2N_{12}Ni_2O_8$ (921.2): calcd. C 40.42, H 7.00, N 18.25; found C 39.95, H 7.07, N 17.40.

Complex 6·$(ClO_4)_2$: A solution of **1**·$(ClO_4)_2$ (0.44 g, 0.50 mmol) in EtOH/THF (1:1, 25 mL) was treated with five equivalents of cnge and stirred at room temperature for 2 h. All volatile material was then evaporated under reduced pressure, the residue taken up in acetone and again treated with three equivalents of cnge. Layering the resulting solution with light petroleum gradually afforded green crystals of the product **6**·$(ClO_4)_3$·acetone (0.11 g, 0.09 mmol, 19%). – IR (KBr): $\tilde{\nu}$ = 3433 (m), 3343 (m), 3238 (m), 2963 (m), 2877 (w), 2233 (s), 2186(s), 1699 (m, acetone), 1641 (s), 1565 (s), 1464 (m), 1259 (m), 1086 (vs), 796 (m), 623 (s) cm^{-1}. – $C_{33}H_{69}Cl_3N_{16}Ni_2O_{12}$·acetone (1163.8): calcd. C 37.15, H 6.50, N 19.26; found C 37.45, H 6.49, N 20.03.

Complex 7·(ClO_4)·(BPh_4): A solution of HL (0.17 g, 0.54 mmol) in EtOH/THF (20 mL, 1:1) was treated with $[Ni(H_2O)_6](ClO_4)_2$ (0.20 g, 0.54 mmol) and cnge (0.05 g, 0.60 mmol) and the reaction mixture stirred for 1 h at room temperature. Then $NaBPh_4$ (0.19 g, 0.56 mmol) was added and the resulting solution layered with light petroleum. Green crystals of **7**·(ClO_4)·(BPh_4)·0.5thf·0.18EtOH

Table 4. Crystal data and refinement details for complexes **4**·$(ClO_4)_2$, **5**·$(ClO_4)_2$, **6**·$(ClO_4)_3$, **7**·(ClO_4)·(BPh_4) and **8**·$(ClO_4)_2$

	4·$(ClO_4)_2$	**5**·$(ClO_4)_2$	**6**·$(ClO_4)_3$	**7**·$(ClO_4)(BPh_4)$	**8**·$(ClO_4)_2$
Formula	$C_{30}H_{62}Cl_2N_{10}Ni_2O_8$	$C_{31}H_{63}Cl_2N_{12}Ni_2O_8$	$C_{33}H_{69}Cl_3N_{16}Ni_2O_{12}$ ·acetone	$C_{36}H_{65}Cl_2N_9Ni_2O_9$· 0.5thf·0.18EtOH	$C_{36}H_{65}Cl_2N_9Ni_2O_9$
M_r	879.2	921.2	1163.9	915.3	956.3
crystal size [mm]	0.03 × 0.15 × 0.30	0.20 × 0.15 × 0.08	0.30 × 0.20 × 0.20	0.08 × 0.30 × 0.30	0.30 × 0.30 × 0.40
crystal system	monoclinic	triclinic	monoclinic	triclinic	monoclinic
space group	*Cc*	$P\bar{1}$	$P2_1/n$	$P\bar{1}$	*C*2/c
a [Å]	8.473(2)	11.474(2)	21.046(4)	10.714(2)	34.338(7)
b [Å]	23.895(5)	12.391(3)	11.178(2)	11.484(2)	9.989(2)
c [Å]	19.412(4)	15.839(3)	24.241(5)	21.713(4)	26.357(5)
α [°]	90	106.40(3)	90	81.06(3)	90
β [°]	90.86(3)	90.77(3)	110.77(3)	89.50(3)	105.40(3)
γ [°]	90	102.27(3)	90	76.35(3)	90
V [Å^3]	3930(1)	2104(1)	5332(1)	2564(1)	8716(3)
$\rho_{calcd.}$ [g·cm^{-3}]	1.486	1.454	1.450	1.184	1.458
Z	4	2	4	2	8
F(000) [e]	1864	976	2456	971	4048
T [K]	200	200	200	200	200
μ (Mo-K_α) [mm^{-1}]	1.154	1.082	0.928	0.479	1.048
hkl range	±10, ±29, ±23	±14, ±15, ±19	–27 to 28, –15 to 14, –34 to 31	±14, ±15, ±29	±42, ±12, ±32
2θ range [°]	3.4−52.2	3.5−52.2	3.6–61.1	3.9−57.4	3.2−52.0
Measured refl.	7791	41676	49853	25867	66921
Unique refl. (*R*int)	7677 (0.084)	8285 (0.069)	14533 (0.089)	13198 (0.079)	8549 (0.088)
Obs. refl. $I > 2\sigma(I)$	6024	5598	7878	6505	6165
refined parameters	505	519	663	664	534
resid. electron dens. [eÅ^{-3}]	0.503/–0.437	0.435/–0.354	0.529/–0.460	0.800/–0.398	1.034/–0.505
R1	0.062	0.039	0.046	0.068	0.042
wR2 (refinement on F^2)	0.142	0.077	0.112	0.230	0.106
Goodness-of-fit	1.029	0.961	0.967	1.016	1.039

gradually formed (0.33 g, 0.36 mmol, 67%). – IR (KBr): $\tilde{\nu}$ = 3421 (s), 3343 (s), 3234 (m), 3046 (m), 2976 (m), 2874 (w), 2227 (s), 2183 (s), 1636 (s), 1550 (s), 1472 (m), 1095 (s), 734 (s), 706 (s) cm^{-1}. – MS (FAB, nibeol); *m*/*z* (%): 466 (44) [$LNi(ClO_4)^+$], 450 (17) [**7**$^+$], 366 (100) [LNi^+]. – $C_{43}H_{59}BClN_9NiO_4$·0.5thf·0.18EtOH (915.3): calcd. C 59.52, H 7.06, N 13.77; found C 58.52, H 7.42, N 13.86.

Complex 8·$(ClO_4)_2$: A solution of **1**·$(ClO_4)_2$ (0.35 g, 0.40 mmol) in EtOH/THF (1:1, 15 mL) was treated with one equivalent of 2-hydroxybenzonitrile (0.048 g, 0.40 mmol) and stirred at room temperature for 1 h. All volatile material was then evaporated under reduced pressure and the residue taken up in acetone and layered with light petroleum. Green crystals of the product **8**·$(ClO_4)_2$ gradually formed (0.31 g, 0.32 mmol, 81%). – IR (KBr): $\tilde{\nu}$ = 2972 (m), 2875 (m), 2237 (s), 1594 (s), 1527 (w), 1476 (s), 1379 (w), 1092 (vs) cm^{-1}. – MS (FAB, nibeol); *m*/*z* (%): 857 (100) [**8**·$(ClO_4)^+$], 755 (90) [**8**$^+$], 378 (65) [**8**$^{2+}$]. – $C_{36}H_{65}Cl_2N_9Ni_2O_9$ (956.3): calcd. C 45.22, H 6.85, N 13.18; found C 44.84, H 6.92, N 12.95.

Calculation Details: The calculations were carried out with the density functional theory method (DFT) known in the literature by its synonym B3LYP.[26] A single extended all-electron basis set was applied in our studies. For Ni we have chosen Wachters (14s,9p,5d) basis set[27] augmented with a 4f polarization function (α_f = 1.29). The contraction scheme of [9s,5p,3d,1f] corresponds to a double- and triple-ζ basis for the core and valence electrons, respectively. The 6–311G basis[28] was used for C, N, and H. The basis set of C and N was augmented by a single 3d polarization function (α_C = 0.626, α_N = 0.913). The geometry optimizations were carried out by using analytical gradient procedures. The presented structures correspond to fully converged geometries with gradients and displacements below the thresholds implemented in Gaussian 98. Vibrational frequencies were obtained from analytic calculations of the Hessian matrices. The calculated frequencies have been scaled by a factor of 0.96. The nature and extent of charge reorganizations was characterized with the help of the natural population analysis (NPA) and natural bond orbital (NBO) methods.[29] The calculations have been carried out with the Gaussian 98 program[30] installed on the IBM RS/6000 workstations of the Universitätsrechenzentrum Heidelberg. For graphical displays we have used the Molek-9000,[31] and GaussView[32] programs.

X-ray Crystallography: The measurements were carried out on a Nonius Kappa CCD diffractometer using graphite-monochromated Mo-K_α radiation. All calculations were performed using the SHELXT PLUS software package. Structures were solved by direct methods with SHELXS-97 and refined with the SHELXL-97 program.[33] The program XPMA[34] was used for graphical handling of the data. Atomic coordinates and thermal parameters of the nonhydrogen atoms were refined in fully or partially anisotropic models by full-matrix least-squares calculation based on F^2. In general the hydrogen atoms were placed at calculated positions and allowed to ride on the atoms they are attached to. The structure of **4**·$(ClO_4)_2$ was treated as a racemic twin. The hydrogen atom H200 of the $HNCN^-$ bridge was located in the difference Fourier synthesis and refined isotropically. In the case of **5**·$(ClO_4)_2$ all hydrogen atoms of the monodeprotonated cnge ligand (H50 – H52) were located and refined. Likewise, for **6**·$(ClO_4)_3$ the protons H22 – H25 and H122 – H125 of the two cnge ligands were located in the difference Fourier map, refined once and then held fixed. One of the terminal ethyl groups (C10 and C14) of **6**·$(ClO_4)_3$ was found to be disordered over two positions (ratio 50:50). In the case of **7**·$(ClO_4)(BPh)_4$ the cnge ligand was found to be partly disordered over two positions (ratio 85:15). The pyrazol-H2 could be found and refined; hydrogen atoms H102, H112, H103, H113 corresponding to the major part of the disordered cnge were located, refined

once and then held fixed. Table 4 compiles the data for the structure determinations. Crystallographic data (excluding structure factors) for the structures reported in this paper have been deposited with the Cambridge Crystallographic Data Centre as supplementary publication no. CCDC 127490 – CCDC-127493 and CCDC-133913. Copies of the data can be obtained free of charge on application to CCDC, 12 Union Road, Cambridge CB2 1EZ, UK [Fax: (internat.) + 44-1223/336-033; E-mail: deposit@ccdc.cam.ac.uk].

Acknowledgments

We sincerely thank Prof. Dr. G. Huttner and Prof. Dr. R. Gleiter for their generous support. Financial support of this work by the Deutsche Forschungsgemeinschaft (SFB 247, Habilitandenstipendium for F. M.) and the Fonds der Chemischen Industrie is gratefully acknowledged.

[1] K. D. Karlin, *Science* **1993**, *261*, 701–708; S. J. Lippard, J. M. Berg, *Principles of Bioinorganic Chemistry*, University Science Books, CF, **1994**; W. Kaim, B. Schwederski, *Bioanorganische Chemie*, Teubner, Stuttgart, **1991**; *Bioinorganic Catalysis* (Ed.: J. Reedijk), Dekker, New York, **1993**; N. Sträter, W. N. Lipscomb, T. Klabunde, B. Krebs, *Angew. Chem.* **1996**, *108*, 2158–2191; *Angew. Chem. Int. Ed. Engl.* **1996**, *35*, 2024–2055.

[2] R. M. Bullock, C. P. Casey, *Acc. Chem. Res.* **1987**, *20*, 167–173; H. Steinhagen, G. Helmchen, *Angew. Chem.* **1996**, *108*, 2489–2492; *Angew. Chem. Int. Ed. Engl.* **1996**, *35*, 2339–2342; D. G. McCollum, B. Bosnich, *Inorg. Chim. Acta* **1998**, *270*, 13–19; E. K. van den Beuken, B. L. Feringa, *Tetrahedron* **1998**, *54*, 12985–13011; R. Than, A. A. Feldmann, B. Krebs, *Coord. Chem. Rev.* **1999**, *182*, 211–241.

[3] M. W. Göbel, *Angew. Chem.* **1994**, *106*, 1201–1203; *Angew. Chem. Int. Ed. Engl.* **1994**, *33*, 1141; M. E. Broussard, B. Juma, S. G. Train, W. J. Peng, S. A. Laneman, G. G. Stanley, *Science* **1993**, *260*, 1784–1788; G. Süss-Fink, *Angew. Chem.* **1994**, *106*, 71–73; *Angew. Chem. Int. Ed. Engl.* **1994**, *33*, 67.

[4] See for example: S. R. Collinson, D. E. Fenton, *Coord. Chem. Rev.* **1996**, *148*, 19–40; D. E. Fenton, H. Okawa, *Chem. Ber./Recueil* **1997**, *130*, 433–442.

[5] F. Meyer, K. Heinze, B. Nuber, L. Zsolnai, *J. Chem. Soc., Dalton Trans.* **1998**, 207–213; F. Meyer, A. Jacobi, B. Nuber, P. Rutsch, L. Zsolnai, *Inorg. Chem.* **1998**, *37*, 1213–1218; M. Konrad, F. Meyer, K. Heinze, L. Zsolnai, *J. Chem. Soc., Dalton Trans.* **1998**, 199–205; F. Meyer, P. Rutsch, *Chem. Commun.* **1998**, 1037–1038.

[6] F. Meyer, H. Pritzkow, *Chem. Commun.* **1998**, 1555–1556.

[7] F. Meyer, E. Kaifer, P. Kircher, K. Heinze, H. Pritzkow, *Chem. Eur. J.* **1999**, *5*, 1617–1630.

[8] L. M. Estermaier, A. H. Sieber, F. Lottspeich, D. H. M. Matern, G. R. Hartmann, *Angew. Chem.* **1992**, *104*, 655–658; *Angew. Chem. Int. Ed. Engl.* **1992**, *31*, 620.

[9] R. W. Miller, R. R. Eady, *Biochim. Biophys. Acta* **1988**, *952*, 290–296.

[10] W. Beck, H. Bock, R. Schlodder, *Z. Naturforsch.* **1974**, *29b*, 75–79.

[11] P. Chauduri, K. Wieghardt, B. Nuber, J. Weiss, *J. Chem. Soc., Chem. Commun.* **1985**, 265–266.

[12] H. Beyer, W. Walter, *Lehrbuch der Organischen Chemie*, S. Hirzel Verlag, Stuttgart, **1988**, p 368.

[13] I. W. Bassi, C. Benedicenti, M. Calcaterra, R. Intrito, G. Rucci, C. Santini, *J. Organomet. Chem.* **1978**, *144*, 225–237; D. Walther, H. Schönberg, E. Dinjus, J. Sieler, *J. Organomet. Chem.* **1987**, *334*, 377–388; J. Sieler, D. Walther, O. Lindquist, L. Andersen, *Z. Anorg. Allg. Chem.* **1988**, *560*, 119–127.

[14] H. Bock, *Angew. Chem.* **1962**, *74*, 695; H. Bock, H. tom Dieck, *Chem. Ber.* **1966**, *99*, 213–226; K. Krogmann, R. Mattes, *Angew. Chem.* **1966**, *78*, 1064; *Angew. Chem. Int. Ed. Engl.* **1966**, *5*, 1046.

[15] M. H. Chisholm, F. A. Cotton, M. W. Extine, L. A. Rankel, *J. Am. Chem. Soc.* **1978**, *100*, 807–811; M. H. Chisholm, J. C. Huffman, N. S. Marchant, *J. Am. Chem. Soc.* **1983**, *105*, 6162–6163; M. H. Chisholm, J. C. Huffman, N. S. Marchant, *Organometallics* **1987**, *6*, 1073–1080; D. M. Hoffman, S. Lee, *Inorg. Chem.* **1992**, *31*, 2675–2676; T. C. Wright, G. Wilkinson, M. Motevalli, M. B. Hursthouse, *J. Chem. Soc., Dalton Trans.* **1986**, 2017–2019; F. J. G. Alonso, M. G. Sanz, V. Riera, A. A. Abril, A. Tiripicchio, F. Ugozzoli, *Organometallics* **1992**, *11*, 801–808; F. A. Cotton, S. C. Haefner, A. P. Sattelberger, *Inorg. Chim. Acta* **1997**, *266*, 55–63.

[16] W. Sacher, U. Nagel, W. Beck, *Chem. Ber.* **1987**, *120*, 895–900; J. Pickardt, B. Kuhn, *Z. Kristallogr.* **1995**, *210*, 901.

[17] M. Fernanda, N. N. Carvalho, A. J. L. Pombeiro, A. Hills, D. L. Hughes, R. L. Richards, *J. Organomet. Chem.* **1993**, *469*, 179–187.

[18] M. J. Begley, P. Hubberstey, P. H. Walton, *J. Chem. Soc., Chem. Commun.* **1989**, 502–503.

[19] M. J. Begley, P. Hubberstey, P. H. Walton, *J. Chem. Soc., Dalton Trans.* **1995**, 957–962.

[20] M. J. Begley, O. Eisenstein, P. Hubberstey, S. Jackson, C. E. Russell, P. H. Walton, *J. Chem. Soc., Dalton Trans.* **1994**, 1935–1942; M. J. Begely, P. Hubberstey, C. E. Russell, P. H. Walton, *J. Chem. Soc., Dalton Trans.* **1994**, 2483–2488; A. J. Blake, P. Hubberstey, W.-S. Li, C. E. Russel, B. J. Smith, L. D. Wraight, *J. Chem. Soc., Dalton Trans.* **1998**, 647–655.

[21] L. A. Sheludyakova, E. V. Sobolev, A. V. Arbuznikow, E. B. Burgina, L. I. Kozhevina, *J. Chem. Soc., Faraday Trans.* **1997**, *93*, 1357–1360.

[22] F. L. Hirshfeld, H. Hope, *Acta Crystallogr.* **1980**, *B36*, 406–415.

[23] C. J. O'Connor, *Progr. Inorg. Chem.* **1982**, *29*, 203–283; O. Kahn, *Molecular Magnetism*, VCH Publishers, New York, **1993**.

[24] I. Hyla-Kryspin, J. Koch, R. Gleiter, T. Klettke, D. Walther, *Organometallics* 1**998**, *17*, 4724–4733.

[25] B. N. Storhoff, H. C. Lewis, Jr., *Coord. Chem. Rev.* **1977**, *23*, 1–29; R. Hoti, Z. Mihalić, H. Vančik, *Croat. Chem. Acta* **1995**, *68*, 359–371.

[26] A. D. Becke, *J. Chem. Phys.* **1992**, *96*, 2155–2160; *J. Chem. Phys.* **1993**, *98*, 5648–5652; S. H. Vosko, L. Wilk, M. Nusair, *Can. J. Phys.* **1980**, *58*, 1200–1211; C. Lee, W. Yang, R. G. Parr, *Phys. Rev. B* **1988**, *37*, 785–789.

[27] A. J. H. Wachters, *J. Chem. Phys.* **1970**, *52*, 1033–1036.

[28] R. Krishnan, J. S. Binkley, R. Seeger, J. A. Pople, *J. Chem. Phys.* **1980**, *72*, 650–654.

[29] J. P. Foster, F. Weinhold, *J. Am. Chem. Soc*. **1980**, *102*, 7211–7218; A. E. Reed, F. Weinhold, *J. Chem. Phys.* **1983**, *78*, 4066–4073; A. E. Reed, R. B. Weinstock, F. Weinhold, *J. Chem. Phys.* **1985**, *83*, 735–746; A. E. Reed, L. A. Curtiss, F. Weinhold, *Chem. Rev.* **1988**, *88*, 899–926.

[30] M. J. Frisch, G. W. Trucks, H. B. Schlegel, G. E. Scuseria, M. A. Robb, J. R. Cheeseman, V. G. Zakrzewski, J. A. Montgomery, Jr., R. E. Stratmann, J. C. Burant, S. Dapprich, J. M. Millam, A. D. Daniels, K. N. Kudin, M. C. Strain, O. Farkas, J. Tomasi, V. Barone, M. Cossi, R. Cammi, B. Mennucci, C. Pomelli, C. Adamo, S. Clifford, J. Ochterski, G. A. Petersson, P. Y. Ayala, Q. Cui, K. Morokuma, D. K. Malick, A. D. Rabuck, K. Raghavachari, J. B. Foresman, J. Cioslowski, J. V. Otitz, B. B. Stefanov, G. Liu, A. Liashenko, P. Piskorz, I. Komaromi, R. Gomperts, R. L. Martin, D. J. Fox, T. Keith, M. A. Al-Laham. C. Y. Peng, A. Nanayakkara, C. Gonzales, M. Challacombe, P. M. W. Gill, B. Johnson, W. Chen, M. W. Wong, J. L. Andres, M. Head-Gordon, E. S. Replogle, and J. A. Pople, *Gaussian 98 Revision A.5*, Gaussian, Inc., Pittsburgh, PA, **1998**.

[31] P. Bischof, *Molek-9000*, Universität Heidelberg, **1998**.

[32] GaussView, Gaussian, Inc., Pittsbourgh, PA, **1998**.

[33] G. M. Sheldrick, *SHELXL-97, Program for Crystal Structure Refinement*, Universität Göttingen, **1997**; *SHELXS-97, Program for Crystal Structure Solution*, Universität Göttingen, **1997**.

[34] L. Zsolnai, G. Huttner, *XPMA*, Universität Heidelberg, **1998**; http://www.rzuser.uni-heidelberg.de/≈v54/xpm.html.

Received September 29, 1999
[I99341]